Collective dynamics in a disparate mass molten alloy Li_4Tl: Analysis within the approach of generalized collective modes

Taras Bryk[1,2] and J.-F. Wax[3]

[1]*Institute for Condensed Matter Physics, National Academy of Sciences of Ukraine, 1 Svientsitskii Street, UA-79011 Lviv, Ukraine*

[2]*Institute of Applied Mathematics and Fundamental Sciences, National Polytechnic University of Lviv, UA-79013 Lviv, Ukraine*

[3]*Laboratoire de Physique des Milieux Denses, Université Paul Verlaine Metz, 1 Boulevard Arago, 57078 Metz Cedex 3, France*

(Received 12 June 2009; revised manuscript received 2 October 2009; published 24 November 2009)

We report a molecular dynamics (MD) study of collective dynamics in molten Li_4Tl alloy, which was studied experimentally by inelastic neutron-scattering experiments and is supposed to have "fast sound" excitations because of a large ratio of components masses. Time-correlation functions obtained in MD simulations are analyzed by the generalized collective modes approach, that enables to obtain dispersion and damping of the different collective modes, and to estimate their contributions to the time-correlation functions and their corresponding dynamic-structure factors. We show, that there exists a transition in the contributions from the high- and low-frequency branches of collective excitations to the total dynamic-structure factor for wave numbers k around 0.4 $Å^{-1}$. Only the low-frequency hydrodynamic acoustic modes without any fast sound define the Brillouin peak in the long-wavelength range, while the high-frequency modes mainly contribute to the side peak of the total dynamic-structure factor for $k>0.4$ $Å^{-1}$.

DOI: 10.1103/PhysRevB.80.184206 PACS number(s): 61.25.Mv, 61.20.Ja, 61.20.Lc, 62.60.+v

I. INTRODUCTION

Theoretical studies of collective dynamics in liquid alloys with disparate masses are of great interest because of the longstanding issue of the existence of "fast sound" excitations. The existence of such excitations was suggested in 1986 (Ref. 1) on the basis of molecular dynamics (MD) simulations of molten Li_4Pb alloy with 250 particles. The calculated partial dynamic-structure factor $S_{\mathrm{LiLi}}(k,\omega)$, where k and ω are the wave number and frequency, respectively, revealed a high-frequency side peak down to the smallest accessible wave number. This peak was interpreted as a collective excitation supposedly propagating via the light component of the molten alloy. Because of a rather small simulated system size, there was no answer to how the dispersion of these specific collective modes would behave in the $k\to 0$ limit. Later on, a similar behavior of the high-frequency collective modes was observed in several gas mixtures, namely, He-Xe,[2] He-Ne,[3] and He-Ar.[4] Fast sound became a widely used name for exotic collective excitations whose phase speed several times exceeds the hydrodynamic speed of sound, although there were still no clue to what is really the long-wavelength asymptote of the fast sound dispersion.

Inelastic neutron-scattering (INS) experiments conducted in 1994 on molten Li_4Pb and Li_4Tl (Ref. 5) obtained the first experimental evidence of the existence of collective modes with a phase speed much higher than the hydrodynamic speed of sound in liquid metallic alloys. The lowest wave numbers accessible in these INS experiments was $k\approx 10$ nm^{-1}. However, the issue of the long-wavelength behavior of the high-frequency branch remained open and was formulated as follows: does the fast sound merge with the hydrodynamic sound mode or does it disappear at approaching the hydrodynamic region?

In 1997, new accurate INS experiments were performed on molten Li_4Pb at 1075 K,[6] which supported previous results about the existence of high-frequency excitations with a phase speed ≈ 4500 m/s, while the hydrodynamic speed of sound, c_s, is only ≈ 2100 m/s. However, in that report, the authors associated the observed high-frequency modes with localized atomic motions of particles of different species with opposite phases and not with the propagation of acoustic modes. But, a few months later, the same group presented results of numerical analysis of the peak positions of partial current spectral functions obtained from MD-derived time-correlation functions.[7] Contrary to their former hypothesis, these results showed two branches of collective excitations merging for $k<0.111$ $Å^{-1}$ into the hydrodynamic linear dispersion law, $\omega=c_s k$.

Very similar results had been obtained a few years before by the same methodology in the case of a gas mixture, $He_{0.8}Ne_{0.2}$.[8] It had been observed that both low- and high-frequency branches merged into a linear dispersion for wave numbers $k<0.07$ $Å^{-1}$. At this point, one has to realize that the estimation of the dispersion of two branches of collective excitations $\omega_i(k)$, $i=1,2$ in binary liquids from side peak positions of partial dynamic-structure factors, $S_{ii}(k,\omega)$, or of spectral functions of partial longitudinal currents, $C^L_{ii}(k,\omega)$ is an intuitive extension of the methodology widely used in pure fluids. Such a numerical approach makes only sense if cross-correlations between species do not exist or are very weak. This is not the case in the long-wavelength range, where the cross-correlations between partial densities are quite strong, especially in liquid alloys with disparate masses. In 2000, considering the contributions from low- and high-frequency branches to the spectral functions of partial transverse current, it was clearly shown[9] that partial spectral functions cannot be used to correctly estimate the dispersion of both branches in the long-wavelength range.

To date, there are mainly two different interpretations of fast sound dispersion in the long-wavelength limit. The first one follows from the purely numerical analysis of partial spectral functions and states that both the low- and high-

frequency branches merge into a single hydrodynamic acoustic branch below some small wave number. The second interpretation of the fast sound is based on an analytical theory,[10] which states that the high-frequency branch corresponds to *nonhydrodynamic* opticlike excitations with contribution to the dynamic-structure factors vanishing in the long-wavelength range. Indeed, when performing a purely numerical analysis of side peak positions of $S_{ij}(k,\omega)$, this vanishing contribution can yield an effect of rapidly decaying dispersion law of high-frequency excitations towards the long-wavelength limit. The specific feature of all nonhydrodynamic collective processes (such as structural relaxations, opticlike modes, heat waves, etc.) is their vanishing contributions to all dynamic-structure factors in the long-wavelength region. In the case of Li_4Pb,[11,12] it was shown that the range of wave numbers where one can definitely say that the high- and low-frequency branches correspond to the optic and acoustic collective excitations is very narrow for liquid alloys with disparate masses. For larger wave numbers, the branches reflect "partial" dynamics of light and heavy subsystems with comparable damping. The necessary conditions for the existence of longitudinal[10] and transverse[9] opticlike modes in binary liquids explain why the high-frequency branch does not exist in the long-wavelength region in the cases of gaseous mixtures such as He-Ne and He-Ar. Therefore, their dispersions tend to zero at some nonzero wave number as it was obtained in kinetic theory.[13] The existence of opticlike excitations was also supported by the memory-function approach, developed for binary liquids in Refs. 14 and 15. One may treat the rapidly decaying and vanishing at some nonzero wave-number dispersion of the high-frequency branch as another example of fast sound. However, the microscopic mechanism leading to this specific behavior of the high-frequency branch is completely explained by the theory of opticlike modes and conditions of their existence in liquids.[9,10]

One also has to mention here the simulation studies of collective dynamics in two-component fcc disordered crystals[16] and polycrystals[17] with disparate masses. In both cases, contributions from the high-frequency optic modes to the dynamic-structure factors were observed. However, essential differences exist between the collective dynamics of these solid systems and binary liquids. In disordered crystals and polycrystals, the viscous regime is completely absent in the long-wavelength range and can thus not be directly compared with the dynamics in liquids at these wavelengths. Opticlike excitations in binary liquids have finite nonzero damping in the long-wavelength limit that almost excludes the possibility to recover these collective excitations in the shape of dynamic-structure factors in the viscous regime.

Molten Li_4Pb was the most intensively studied by the molecular-dynamics simulations among all the fast sound liquid systems. On the other hand, there are no available simulation results of collective dynamics of molten Li_4Tl, which is another fast sound system studied by INS experiments.[5] This is mainly due to the difficulties encountered in describing accurately the effective interionic interactions in this melt. Indeed, accurate models of interactions for polyvalent metals are scarce in the literature in comparison to alkali metals. In this study, we have used Fiolhais

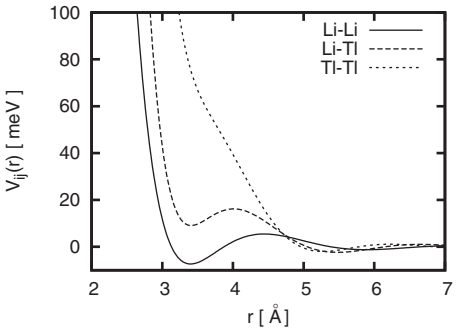

FIG. 1. Effective pair potentials for molten Li_4Tl obtained from Fiolhais pseudopotentials.

pseudopotential[18] to obtain two-body effective potentials for molten Li_4Tl. This model has proved to produce correct density-dependent effective potentials for molten Li (Ref. 19) and molten Tl.[20] It was also successful in the case of some alloys.[21]

Our aim was not only to simulate molten Li_4Tl and calculate dynamic-structure factors but also to apply a careful analysis of different time-correlation functions and to find out which of the dynamic models can describe correctly the dispersion branches of collective excitations in this fast sound liquid system. The correct mechanisms of fast sound dispersion can only be revealed in such a detailed study of collective dynamics. The analysis of time-correlation functions of molten Li_4Tl obtained in MD simulations was performed by the generalized collective modes (GCM) approach with explicit treatment of thermal fluctuations. On the basis of numerous analytical and numerical results for pure and binary liquids, this is to date the most advanced method of exploration of hydrodynamic and nonhydrodynamic collective excitations in liquids. So, this paper is organized as follows. In the next section, our MD simulations and theoretical scheme of analysis of collective dynamics are detailed. In the third section, we report Bhatia-Thornton static structure factors and generalized thermodynamic quantities, as well as dispersion and damping of low- and high-frequency branches of collective excitations. We also examine the wave-number-dependent contributions from the collective excitations to different dynamic-structure factors, that clearly reflect the expected long-wavelength asymptotes for the spectrum and total dynamic-structure factor. Conclusions of this study will be given in the last section.

II. DETAILS OF MD SIMULATIONS AND METHOD OF ANALYSIS OF COLLECTIVE DYNAMICS

The effective two-body potentials for Li_4Tl were obtained from the second-order perturbation theory in pseudopotentials (effective electron-ion interactions) by making use of Fiolhais[18] local pseudopotentials and Ichimaru-Utsumi[22] local field correction. Relevant expressions can be found in Ref. 21. The effective potentials used in this MD study are shown in Fig. 1. They display so-called Friedel long-range oscillations, which are typical for metallic systems. The ranges of the repulsive parts of this set of potentials suggest

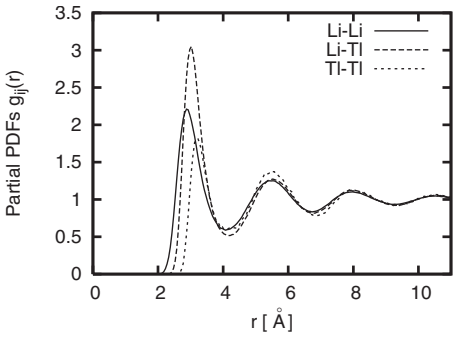

FIG. 2. Partial pair distribution functions of molten Li_4Tl at the thermodynamic point of INS experiment.

that Tl atoms will rather be surrounded by Li ones since the first minimum of $V_{TlTl}(r)$ is shifted to distances corresponding to the second-neighbor distance. It means that this alloys may exhibit heterocoordination tendencies.

MD simulations of Li_4Tl were performed on a model system of 4000 particles with numerical density 0.04625 $Å^{-3}$ using a cubic box subject to periodic boundary conditions. The effective two-body potentials $V_{ij}(r)$ were cutoff at corresponding nodes, located approximately at $R_{cut}=20$ Å. A chain of three Nose-Hoover thermostats were used to keep the mean temperature at the experimental value of 753 K. The timestep was 1.5 fs and the production run 600 000 timesteps long. Every sixth configurations were used to estimate static and dynamic quantities. The high number of configurations ensured well-converged static averages and time-correlation functions to be obtained. Seventeen k points were sampled in MD simulations in the range 0.156–3.4 $Å^{-1}$. Additional averages over all possible directions of k vectors with the same length were performed.

Partial pair-distribution functions, $g_{ij}(r)$, for Li_4Tl at 753 K are shown in Fig. 2. As expected for the smallest particles, Li-Li partial pair distribution has its main maximum at the shortest distance. The sequence of first peak locations are 2.9, 3.02, and 3.21 Å for Li-Li, Li-Tl, and Tl-Tl functions, respectively. According to the height of the first peaks, the heterocoordination tendency clearly appears. Indeed, $g_{LiTl}(r)$ displays the highest one, indicating that pairs of first neighbors of different chemical species are more abundant than in the corresponding random mixture.

In this study, collective dynamics in molten Li_4Tl is analyzed by the GCM approach (its detailed description in the case of binary liquids can be found in Ref. 23) using the following eight-variables dynamic model:

$$\mathbf{A}^{(8)}(k,t) = \{n_A(k,t), n_B(k,t), \times J_A^L(k,t), J_B^L(k,t), \varepsilon(k,t), \dot{J}_A^L(k,t), \dot{J}_B^L(k,t), \dot{\varepsilon}(k,t)\} \quad (1)$$

with A=Li and B=Tl. In Eq. (1), $n_i(k,t)$ are the partial particle densities, $J_i^L(k,t)$, the partial longitudinal mass currents, $\varepsilon(k,t)$, the energy density, and dotted variables are their respective first time derivatives. All dynamic variables of the basis set $\mathbf{A}^{(8)}(k,t)$ were sampled directly in MD simulations and were used to calculate the corresponding static averages

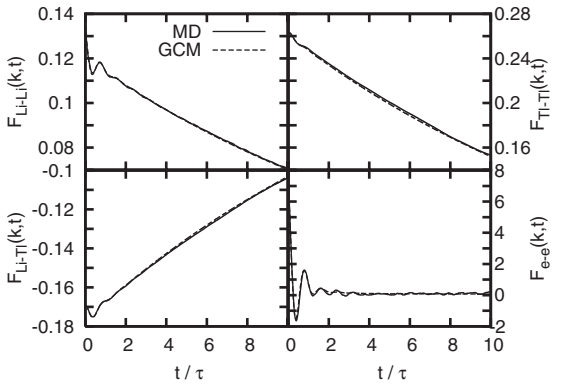

FIG. 3. Partial density-density and energy-energy time-correlation functions at $k=0.156$ $Å^{-1}$, obtained from MD simulations (solid line), and corresponding GCM replicas (dashed lines) for molten Li_4Tl. The time unit τ is equal to 1.74 ps.

and time-correlation functions. An equivalent representation of the dynamic variables of a binary liquid in terms of total $[n_t(k,t)]$ and mass-concentration $[n_x(k,t)]$ densities would lead to identical results within the GCM approach, because both representations [via partial $(A$-$B)$ and $(t$-$x)$ dynamic variables] are connected by linear combinations. The eight dynamic variables of the basis set in Eq. (1) were used to build the 8×8 generalized hydrodynamic matrix, $\mathbf{T}^{(8)}(k)$. Its k-dependent eigenvalues represent the dynamical modes, that can exist in the studied binary liquid. Purely real eigenvalues correspond to nonpropagating relaxation processes, while pairs of complex-conjugated eigenvalues represent propagating modes. One of the most important characteristics of GCM approach is the possibility to represent time-correlation functions between the dynamic variables of the chosen basis set as a separable sum of mode contributions. Consequently, in our study, GCM replicas of the time-correlation functions read

$$F_{ij}^{(8)}(k,t) = \sum_{\alpha=1}^{8} G_{ij}^{\alpha}(k) e^{-z_\alpha(k)t}, \quad (2)$$

where each term corresponds to the contribution from a collective mode $z_\alpha(k)$, and complex weight coefficients $G_{ij}^{\alpha}(k)$ are estimated via corresponding eigenvectors.[23,24] The considered eight-variables dynamic model enables to represent partial density-density time-correlation functions in agreement with up to the fourth frequency moment of corresponding partial dynamic-structure factors $S_{AB}(k,\omega)$, while energy-energy time-correlation function is accurate up to the second frequency moment of $S_{ee}(k,\omega)$. The high quality of GCM replicas can be seen in Fig. 3, where examples of partial density-density and energy-energy time-correlation functions illustrate, how MD-derived functions are well reproduced by the parameter-free expression (2).

III. RESULTS AND DISCUSSION

A. Static-structure factors and generalized thermodynamic quantities

Static wave-number-dependent quantities are very important to understand the role of different microscopic pro-

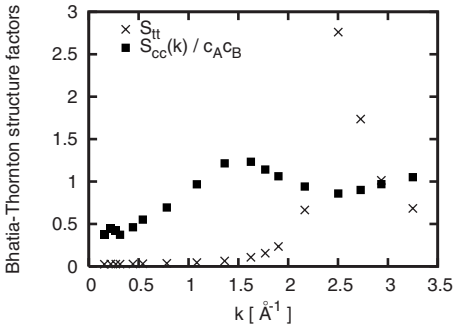

FIG. 4. Bhatia-Thornton static-structure factors for molten Li_4Tl at 753 K.

cesses, such as thermal and viscous ones, on distinct length scales. Among the most widely used wave-number-dependent quantities for the description of structural correlations in binary liquids are the Bhatia-Thornton structure factors $S_{ij}(k)$, $i,j=t,c$, shown in Fig. 4. Indices t and c correspond to total numeric density and concentration density of the binary melt, respectively. Note that the concentration-concentration structure factor has a short-wavelength asymptote equal to c_Ac_B. In the opposite limit, $S_{cc}(k)$ tends to a value noticeably smaller than c_Ac_B. This clear indication of heterocoordination tendencies is fully consistent with our previous mentions of chemical order. Concerning $S_{tt}(k)$, it looks like the static structure factor of a pure liquid since it only accounts for topological order, irrespective of the chemical nature of the atoms. It is different from the total structure factor as measured in neutron or x-ray scattering experiments, which involves atomic scattering form factors. It would have been interesting to compare the simulation predictions with experimental results, but, unfortunately, these latter are not available in the literature. For the subsequent analysis of the dispersion of different branches of collective excitations, it is important to keep in mind that the main peaks of $S_{tt}(k)$ and $S_{cc}(k)$ are located at 2.5 and 1.5 $Å^{-1}$, respectively.

More interesting is the wave-number dependence of generalized thermodynamic quantities (Fig. 5) such as specific heats at constant pressure and volume, $C_P(k)$ and $C_V(k)$, their ratio, $\gamma(k)$, linear thermal-expansion coefficient, $\alpha_T(k)$, dilatation factor, $\delta(k)$, and second derivative of Gibb's energy with respect to concentration at constant pressure, temperature, and number of particles, Z factor.[25] Even in the case of pure liquids, the studies of generalized thermodynamic quantities are very scarce, while for binary liquids such studies were only reported for a couple of systems.[23,26] Their importance lies in the possibility to estimate their long-wavelength limit and, thus, to obtain many thermodynamic quantities directly from MD simulations without any fit. These thermodynamic quantities are essential to analyze the collective dynamics, because contributions from relaxation and propagating collective processes are expressed via thermodynamic quantities and transport coefficients in the hydrodynamic limit.[27]

All the generalized thermodynamic quantities display a pronounced maximum at $k\sim 2.5$ $Å^{-1}$, that coincides with the location of the main peak of the total structural factor $S_{tt}(k)$.

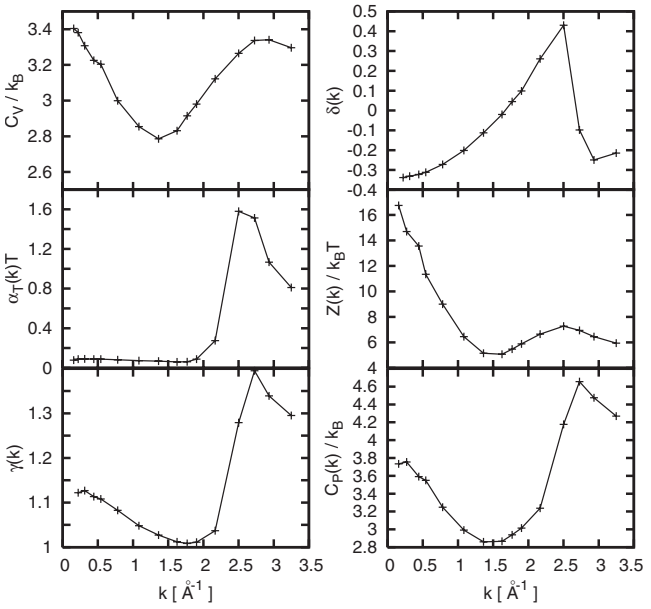

FIG. 5. Generalized thermodynamic coefficients: specific heats at constant volume, $C_V(k)$, and constant pressure, $C_P(k)$, linear thermal expansion coefficient, $\alpha_T(k)$, ratio of specific heats, $\gamma(k)$, dilatation factor, $\delta(k)$, and Z factor for molten Li_4Tl.

Another feature is the minimum of $\gamma(k)$ at $k\sim 1.7$ $Å^{-1}$, where the generalized ratio of specific heats approaches unity. This means that on specific length scales the coupling between thermal and total density fluctuations is very weak. One has to note that all the generalized thermodynamic quantities connected with thermal fluctuations have a minimum in the $k\sim 1.5-2$ $Å^{-1}$ range. The long-wavelength asymptotes of the generalized thermodynamic quantities will be used in next subsections to estimate mode contributions to dynamic-structure factors and Landau-Placzek ratio in molten Li_4Tl.

The generalized thermodynamic quantities and Bhatia-Thornton structure factors ensure to obtain generalized adiabatic speed of sound, $c_s(k)$, for the studied binary melt. According to Ref. 27, the adiabatic speed of sound is

$$c_s(k) = \left[\frac{\gamma(k)}{\rho\kappa_T(k)}\right]^{1/2} \equiv \left[\frac{\gamma(k)k_BT}{\bar{m}[S_{tt}(k) - S_{cc}(k)\delta^2(k)]}\right]^{1/2},$$

where $\kappa_T(k)$ is the generalized wave-number-dependent isothermal compressibility, and $\bar{m}=0.8m_{\mathrm{Li}}+0.2m_{\mathrm{Tl}}$, the average mass. In Fig. 6, we show the calculated wave-number dependence of $c_s(k)$, which tends to a value $c_s=2845$ m s^{-1} in the $k\to 0$ limit. For comparison, the wave-number dependence of the high-frequency speed of sound

$$c_\infty(k) = \frac{1}{k}\left[\frac{\langle \dot{J}_t(-k)\dot{J}_t(k)\rangle}{\langle J_t(-k)J_t(k)\rangle}\right]^{1/2},$$

which is connected to elastic mechanism of sound propagation, is shown in Fig. 6 by line-connected cross symbols. The value obtained in the long-wavelength limit is $c_\infty = 3580$ m s^{-1}. The comparison of both speeds of sound is a standard way to estimate possible "positive dispersion" of

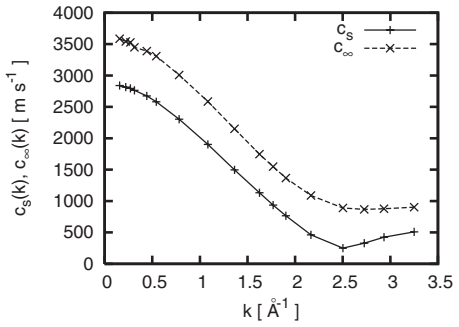

FIG. 6. Generalized adiabatic and high-frequency speeds of sound for molten Li_4Tl.

the acoustic branch[28] due to a crossover between viscous and elastic regimes. It is believed that fast sound in water is, namely, of such origin.[29] However, in the next section we will show that the phase speed of the high-frequency excitations in Li_4Tl is much higher than the expected high-frequency sound. This discards the possibility of a simple viscoelastic mechanism of fast sound in this molten alloy.

B. Spectrum of collective excitations

Two pairs of complex-conjugated eigenvalues

$$z_\alpha(k) = \sigma_\alpha(k) \pm i\omega_\alpha(k), \quad \alpha = 1,2$$

were obtained in the whole range of investigated wave numbers. Here, $\omega_\alpha(k)$ is the dispersion of the αth branch and $\sigma_\alpha(k)$, its damping. In Fig. 7, dispersion and damping of both branches are shown by solid (low-frequency branch) and dashed (high-frequency branch) lines. The dispersion of the low-frequency excitations is quite flat in the $k > 0.5$ Å^{-1} range. For smaller wave numbers, it bends down to match the linear hydrodynamic dispersion law with the same value of c_s as estimated from Fig. 6 and shown by a dotted line. The observed "negative dispersion" of the low-frequency branch as well as the strong positive dispersion of the high-frequency one are consequences of the strong cross-correlations between partial densities on the boundary of hydrodynamic regime in liquids with disparate masses. One can see that the phase speed of the high-frequency collective excitations at this boundary is on the order of 8000 m s^{-1}, that is more than twice as high as the high-frequency speed of sound c_∞ shown in Fig. 6. This excludes the possibility of a simple viscoelastic mechanism for the fast sound in molten Li_4Tl. Like its dispersion, the damping of the low-frequency excitations is almost constant for $k > 0.5$ Å^{-1}, while it transforms into a clear quadratic hydrodynamic dependence, Γk^2 with the sound damping coefficient $\Gamma = 5.4 \times 10^{-7}$ m^2 s^{-1}, towards $k \to 0$.

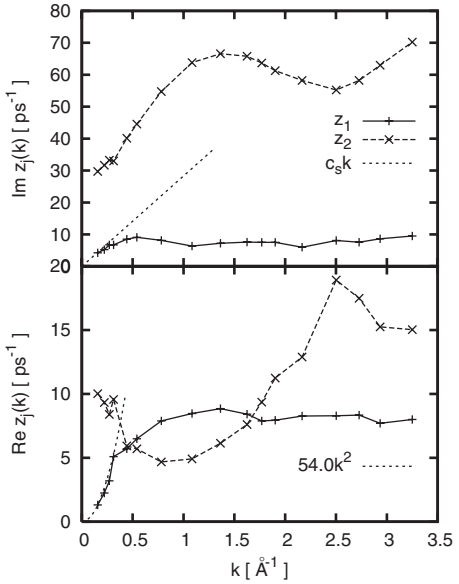

FIG. 7. Dispersion (top frame) and damping (bottom frame) of generalized collective excitations in molten Li_4Tl. Short-dashed lines correspond to the expected hydrodynamic linear asymptote for sound dispersion with $c_s = 2845$ m s^{-1} and to the quadratic asymptote for sound damping with the damping coefficient $\Gamma = 5.4 \times 10^{-7}$ m^2 s^{-1}.

For $k > 0.5$ Å^{-1}, the high-frequency branch behaves typically as a generalized sound dispersion with the minimum at ~ 2.5 Å^{-1}, the location of the main peak of total static structure factor, $S_{tt}(k)$. At this k value, the high-frequency excitations also have their maximum damping, that corresponds to strong scattering on the boundary of the first pseudo-Brillouin zone. More interesting is the long-wavelength domain of the dispersion of the high-frequency branch. Both the frequency and damping tend to finite nonzero values, that are the main features of "kinetic" collective modes, i.e., modes having finite nonzero lifetimes on macroscopic length scales, and which therefore do not survive on macroscopic distances in comparison with the hydrodynamic ones.

In order to estimate the origin of both types of collective excitations in different ranges of wave numbers, we will apply the same procedure as was proposed in Ref. 9. The basis set of eight dynamic variables [Eq. (1)] can be divided into several subgroups characterized by their origin, i.e., two groups of three partial dynamic variables corresponding to both species

$$\mathbf{A}^{(3i)} = \{n_i, J_i^L, \dot{J}_i^L\}, \quad i = \mathrm{Li}, \mathrm{Tl} \tag{3}$$

and another group of two dynamic variables connected with energy fluctuations $\mathbf{A}^{(2e)} = \{\varepsilon, \dot{\varepsilon}\}$. Another possibility is to use linear combinations of partial dynamic variables (see Ref. 9 for details) in order to have two subsets linked with total density fluctuations

$$\mathbf{A}^{(3t)} = \{n_t, J_t^L, \dot{J}_t^L\} \tag{4}$$

and mass-concentration fluctuations

$$\mathbf{A}^{(3x)} = \{n_x, J_x^L, \dot{J}_x^L\}. \tag{5}$$

The complex eigenvalues of the different three-variables dynamic models $\mathbf{A}^{(3i)}$, $i = t, x, \mathrm{Li}, \mathrm{Tl}$ [Eqs. (3)–(5)] can easily be obtained and thus compared with the eigenvalues deduced from the full eight-variables dynamic model, $\mathbf{A}^{(8)}$. This latter takes into account all the local coupling effects between the different subgroups of fluctuations.

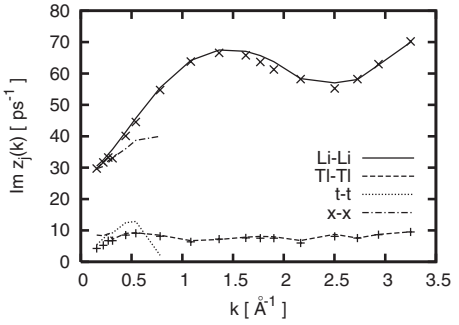

FIG. 8. Analysis of the origin of collective excitations by means of separated subsets of dynamic variables $\mathbf{A}^{(3i)}$, $i=\mathrm{Li},\mathrm{Tl},t,x$ [Eqs. (3)–(5)]. As in the previous figure, symbols correspond to the dispersion of the two branches obtained from the full eight-variables dynamic model. The lines correspond to dispersion of propagating modes obtained from the three-variables dynamic models: only Li-Li correlations (solid line), only Tl-Tl correlations (dashed line), only mass-concentration (x-x) correlations (dash-dotted line), and only total density (t-t) correlations (dotted line).

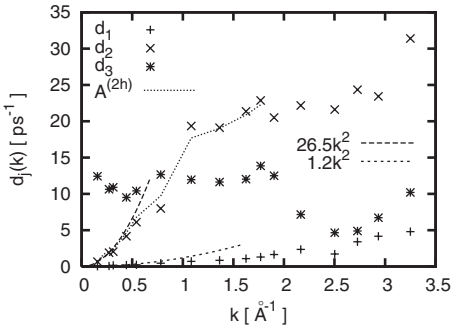

FIG. 9. The three slowest wave-number-dependent relaxation processes obtained as purely real eigenvalues, $d_j(k)$, of the generalized hydrodynamic matrix. Both lowest eigenvalues, $d_1(k)$ and $d_2(k)$, have correct hydrodynamic asymptotes (dashed lines) in the long-wavelength limit and correspond to relaxation processes connected mainly with mutual and thermal diffusivity, respectively. The wave-number dependence of the eigenvalue $d_2(k)$ was distinguished from $d_3(k)$ by considering the lowest heat mode (dotted line) obtained from the only dynamic model $\{h_k,\dot{h}_k\}$ of heat subsystem. The eigenmode $d_3(k)$ corresponds to structural relaxation and is slower than the thermal relaxation process $d_2(k)$ for $k>0.8$ Å^{-1}.

In Fig. 8, the imaginary parts of complex eigenvalues obtained within the eight-variables dynamic model (symbols) are compared with those of the three-variables dynamic models (lines). For $k>0.4$ Å^{-1}, the complex eigenvalues of the eight-variables dynamic model are in perfect agreement with the complex eigenvalues obtained within the three-variables dynamic models $\mathbf{A}^{(3i)}$, $i=\mathrm{Li},\mathrm{Tl}$ [Eq. (3)], representing dynamics of partial type. This means that for $k>0.4$ Å^{-1} the cross-correlations between partial dynamic variables are very small, and collective dynamics of Li_4Tl in that domain can simply be represented as a sum of almost independent partial dynamics of species. For $k<0.4$ Å^{-1}, the cross-correlations between partial variables become much stronger, and the separated treatment of dynamic models with partial variables does not make any sense. It is seen that a complex eigenvalue of the dynamic model $\mathbf{A}^{(3\mathrm{Tl})}$ tends to a nonzero value for $k<0.4$ Å^{-1}. In this domain, the complex eigenvalues are much better reproduced by those obtained within the three-variables dynamic models $\mathbf{A}^{(3i)}$, $i=t,x$ [Eqs. (4) and (5)]. This clearly indicates the origin of the low- and high-frequency excitations in the long-wavelength range as acoustic and optic modes, respectively. The local coupling effects between acoustic and optic modes are slowly vanishing in the long-wavelength limit, while they are very strong for $k>0.4$ Å^{-1}. Hence, from Fig. 8 one can conclude that there is a transition between different types of dynamics at approximately $k\sim 0.4$ Å^{-1}: dynamics of partial type for larger wave numbers and weakly coupled acoustic and optic modes in the long-wavelength range.

C. Nonpropagating wave-number-dependent relaxation processes

The eight-variables dynamic model applied in this study to analyze collective dynamics in molten Li_4Tl alloy leads to four purely real eigenvalues $d_j(k)$ in the whole range of studied wave numbers. In Fig. 9, we show the three lowest real eigenvalues, while the highest one, $d_4(k)$, has such a very short lifetime $[d_4(k)\gg d_j(k)$ for $j=1,3]$ over the whole k range that it does not affect significantly the collective dynamics. Indeed, it is of thermal origin and its contribution to the dynamic-structure factors studied here is extremely small.

In fact, due to coupling effects between the relaxation processes the analytical expressions of hydrodynamic relaxation modes[30] are not so simple as in the case of pure fluids. Nevertheless, if coupling between thermal processes and concentration fluctuations is weak, the real eigenmodes can easily be separated within GCM approach to estimate their origin. We have checked mode contributions to the $F_{xx}(k,t)$ function and found that for Li_4Tl the nonpropagating relaxation mode connected with concentration fluctuations completely defines the shape of the concentration density autocorrelation function in the long-wavelength limit. Consistently, the contribution from the other hydrodynamic relaxation process connected with thermal diffusivity is negligible. Therefore, on the basis of hydrodynamic expressions of $F_{xx}(k,t)$,[27] we can definitely say that the lowest real eigenvalue in the long-wavelength range behaves simply as $d_1(k)=D_{12}k^2$ with the mutual diffusivity $D_{12}=1.2\times 10^{-4}$ cm^2 s^{-1} as estimated from Fig. 9. Hence, the second nonpropagating relaxation process with a k^2 dependence in the long-wavelength range mainly corresponds to the thermal diffusivity process with the eigenvalue[30]

$$d_2(k)=D_T\left(1+\frac{D_{12}\chi_T^2 Z}{TC_P}\right)k^2.$$

In the case of small thermal diffusion ratio χ_T, it turns into $d_2(k)\approx D_T k^2$ with D_T being the thermal diffusivity. The quadratic k^2 dependence of the $d_2(k)$ is clearly seen from Fig. 9, and the estimated value of D_T is 2.65×10^{-7} m^2 s^{-1}. The thermal relaxation process origin of $d_2(k)$ and its behavior as a function of wave numbers beyond the hydrodynamic re-

gime is ascertained by considering the wave-number dependence of the lowest eigenvalue (dotted line in Fig. 9) of a two-variables dynamic model, $\mathbf{A}^{(2h)}=\{h(k,t),\dot{h}(k,t)\}$, which solely takes heat fluctuations into account. Here, $h(k,t)$ is the dynamic variable of heat density, which is orthogonal to the total density and mass-concentration fluctuations in contrast to energy density, and $\dot{h}(k,t)$ is the corresponding extended variable. This additional analysis was necessary to separate both relaxing eigenmodes, $d_2(k)$ and $d_3(k)$, which cross around $k\approx 0.8$ Å^{-1}, and estimate the origin of $d_4(k)$. The nonpropagating relaxation process, $d_3(k)$, clearly tends to a nonzero value in the long-wavelength limit, that is a specific feature of kinetic modes. This implies a much shorter lifetime on macroscopic length scales in comparison with slow hydrodynamic modes. For $k>0.8$ Å^{-1}, the kinetic relaxation process $d_3(k)$ becomes slower than the thermal mode $d_2(k)$, as has also been predicted by analytical theory of wave-number dependence of structural relaxation in liquids.[31]

D. Coherent dynamic-structure factors

The time-correlation functions obtained in MD simulations enable us to calculate the different dynamic-structure factors of interest. We calculated the total coherent neutron-weighted dynamic-structure factor as follows:

$$S_{\mathrm{INS}}(k,\omega)=b_{\mathrm{Li}}^{*2}c_{\mathrm{Li}}S_{\mathrm{LiLi}}(k,\omega)+2b_{\mathrm{Li}}^{*}b_{\mathrm{Tl}}^{*}\sqrt{c_{\mathrm{Li}}c_{\mathrm{Tl}}}S_{\mathrm{LiTl}}(k,\omega)+b_{\mathrm{Tl}}^{*2}c_{\mathrm{Tl}}S_{\mathrm{TlTl}}(k,\omega), \quad (6)$$

where $S_{ij}(k,\omega)$ are the partial dynamic-structure factors, c_i, the corresponding concentrations, and introducing

$$b_i^{*}=\frac{b_i}{\sqrt{c_{\mathrm{Li}}b_{\mathrm{Li}}^2+c_{\mathrm{Tl}}b_{\mathrm{Tl}}^2}},\quad i=\mathrm{Li},\mathrm{Tl}.$$

The values of the coherent scattering lengths of the pure elements, b_i, used in this work are the same as in the analysis of INS experiment.[5]

In Fig. 10, we show the total coherent INS-weighted dynamic structure for two wave numbers, which are in the range investigated by the INS experiments.[5] It is clearly seen that the side peaks of $S_{\mathrm{INS}}(k,\omega)$ are due to contributions from the propagating high-frequency collective modes. This supports the experimental results of Ref. 5 according to which shoulders on the reported experimental scattering intensity in the interval $1<k<1.8$ Å^{-1} are caused by the high-frequency excitations treated as fast sound.

E. Mode contributions to dynamic-structure factors

One of the main advantages of the GCM approach as well as of kinetic theory[13] over the other existing methodologies of analysis of collective dynamics in many-components liquids lies in the possibility to trace the wave-number dependence of mode contributions. It is important that there exist analytical expressions for mode contributions to the density-density time-correlation functions of binary liquids in the hydrodynamic limit.[30] However, the main issue is to determine how these hydrodynamic modes along with nonhydrodynamic processes contribute to the time-correlation functions or corresponding spectral functions beyond the hydrodynamic domain.

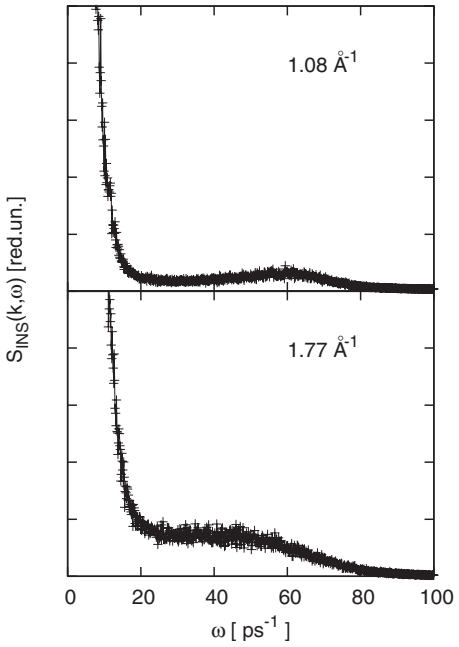

FIG. 10. Neutron-weighted total coherent dynamic-structure factor of liquid Li_4Tl calculated numerically from the MD data for two k values in the range investigated by the INS experiment.

Wave-number-dependent contributions to different dynamic-structure factors in binary liquids can clearly reveal, which branch of the collective excitations is responsible for the side peaks in different ranges of wave numbers. Besides, the analysis of mode contributions to the dynamic-structure factors (or to corresponding time-correlation functions) can reflect possible transitions in the leading contributions to the central or side peaks from different collective processes. Such a transition is, for instance, observed even in the case of pure liquids. It usually takes place at wave numbers $\sim 0.4-0.7$ Å^{-1}, where lifetimes of the hydrodynamic thermal relaxation process and of the structural relaxation become equal. For larger wave numbers, the structural relaxation represents the leading contribution to the central peak of dynamic-structure factor,[26,32] while the thermal diffusivity does as $k\to 0$.

In the case of the binary molten alloy with disparate masses, Li_4Tl, we will focus on mode contributions to the four dynamic-structure factors of main interest: total and mass-concentration dynamic-structure factors [$S_{tt}(k,\omega)$ and $S_{xx}(k,\omega)$, respectively] and partial dynamic-structure factors [$S_{ii}(k,\omega)$, i=Li,Tl]. The general GCM expression for the dynamic-structure factors with complex weights of mode contributions $G_{ij}^{\alpha}(k)$ (Ref. 33) reads

$$S_{ij}(k,\omega)=\mathrm{Re}\left[\sum_{\alpha=1}^{N_v}\frac{G_{ij}^{\alpha}(k)}{i\omega+z_{\alpha}(k)}\right]. \quad (7)$$

Separating the N_{rel} contributions of nonpropagating relaxation processes from the $2N_{prop}$ contributions of propagating processes ($N_{rel}+2N_{prop}=N_v$), this expression is easily trans-

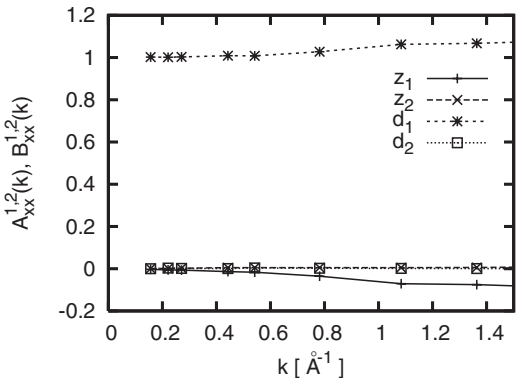

FIG. 11. Wave-number-dependent mode-strengths [Eq. (8)] of generalized collective modes in mass-concentration dynamic-structure factor $S_{xx}(k,\omega)$. The mode strengths $A^1_{xx}(k)$ and $A^2_{xx}(k)$ correspond to the two hydrodynamic relaxation modes $d_1(k)$ and $d_2(k)$. The low- and high-frequency branches of collective excitations, $z_1(k)$ and $z_2(k)$, contribute to the $S_{xx}(k,\omega)$ with the symmetric mode strengths $B^1_{xx}(k)$ and $B^2_{xx}(k)$, respectively.

formed into the following form with real weights (mode strengths):[34]

$$\frac{S_{ij}(k,\omega)}{S_{ij}(k)} = \sum_{\alpha=1}^{N_{rel}} A_{ij}^{\alpha}(k)\frac{2d_{\alpha}(k)}{\omega^2 + d_{\alpha}^2(k)} + \sum_{\pm,\beta=1}^{N_{prop}} \left[B_{ij}^{\beta}(k)\frac{\sigma_{\beta}(k)}{[\omega \pm \omega_{\beta}(k)]^2 + \sigma_{\beta}^2(k)} \pm D_{ij}^{\beta}(k)\frac{\omega \pm \omega_{\beta}(k)}{[\omega \pm \omega_{\beta}(k)]^2 + \sigma_{\beta}^2(k)} \right]. \quad (8)$$

In this expression, wave-number-dependent mode strengths $A_{ij}(k)$ reflect amplitudes of mode-contributions from different nonpropagating relaxation processes (either hydrodynamic or nonhydrodynamic) to the central peak of dynamic-structure factor $S_{ij}(k,\omega)$. The contributions from propagating processes, which form the side peaks of dynamic-structure factors, have a symmetric (Lorentzian) and nonsymmetric (non-Lorentzian) parts with corresponding mode strengths $B_{ij}^{\beta}(k)$ and $D_{ij}^{\beta}(k)$.

The most simple case is the GCM analysis of mode contributions to the mass-concentration dynamic-structure factor $S_{xx}(k,\omega)$. According to hydrodynamic analytic expressions,[27] $S_{xx}(k,\omega)$ does not contain any side peak and consists of two central Lorentzians in case of coupled thermal and mass-concentration fluctuations. The mode contributions to $S_{xx}(k,\omega)$ obtained in a wide range of wave numbers by the GCM approach (Fig. 11) prove that there is only a single contribution from the hydrodynamic mode $d_1(k)$ in the long-wavelength range. The thermal-relaxation mode $d_2(k)$ does not contribute to the central peak of $S_{xx}(k,\omega)$, that indicates a negligible coupling between long-wavelength thermal and concentration fluctuations. Hence, the half width at half height of $S_{xx}(k,\omega)$ at small waven umbers is completely defined by the mutual diffusivity. For wave numbers $k > 0.4$ Å^{-1}, there appears a weak contribution from the low-frequency branch of collective excitations $z_1(k)$. The high-frequency branch $z_2(k)$ does not contribute to $S_{xx}(k,\omega)$. We would like to remind here that according to the analysis performed in previous subsection the absence of coupling between the concentration and thermal fluctuations enabled us to exclusively ascribe the origin of the two lowest relaxation modes, $d_1(k)$ and $d_2(k)$, to nonpropagating relaxation processes connected with mutual diffusivity and thermal conductivity, respectively.

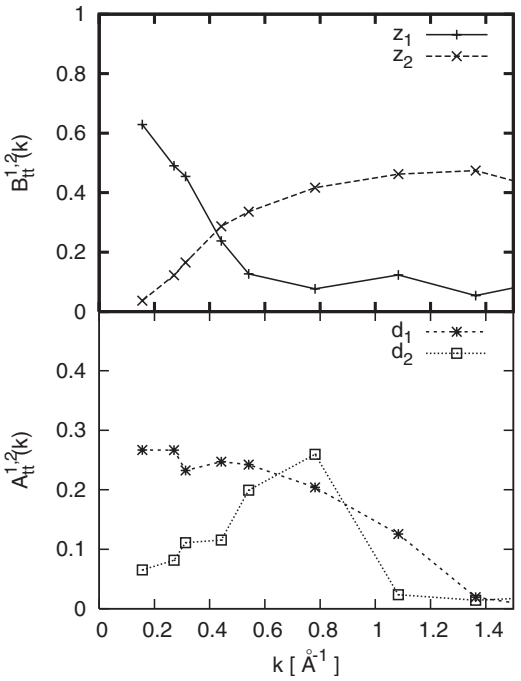

FIG. 12. Wave-number-dependent mode-strengths [Eq. (8)] in the total dynamic-structure factor $S_{tt}(k,\omega)$ of both low- and high-frequency collective excitations (top frame), and of two hydrodynamic relaxation modes (bottom frame). The intersection at about 0.4 Å^{-1} corresponds to a transition in the leading contribution to the dynamic-structure factors from the high- and low-frequency collective modes.

In Fig. 12, the leading mode strengths are shown for the total dynamic-structure factor $S_{tt}(k,\omega)$. In the case of $S_{tt}(k,\omega)$, there only exists an analytical expression in the hydrodynamic limit for the corresponding mode strengths of hydrodynamic modes.[27] Let us recall that the ratio of the integral intensities of the central and side peaks known as the Landau-Placzek ratio is related to the mode strengths. In the case of alloys, it does not simply equal $(\gamma-1)$ as in pure liquids,[27] but

$$\frac{I_{\text{central}}}{2I_{\text{side}}} = \frac{A_{tt}^1 + A_{tt}^2}{B_{tt}} = (\gamma - 1)\left[1 + \frac{\delta^2 C_P}{ZT\alpha_T^2}\right]. \quad (9)$$

Let us first consider the mode strengths of propagating processes in $S_{tt}(k,\omega)$ (their wave-number dependences are shown in the upper frame of Fig. 12). This plot demonstrates that for $k > 0.4$ Å^{-1} the main contribution to the side peak of the total dynamic-structure factor stems from the high-frequency branch $z_2(k)$, which is solely ascribed to the light component of the alloy in this wave-number range according to the analysis performed above. For smaller wave numbers,

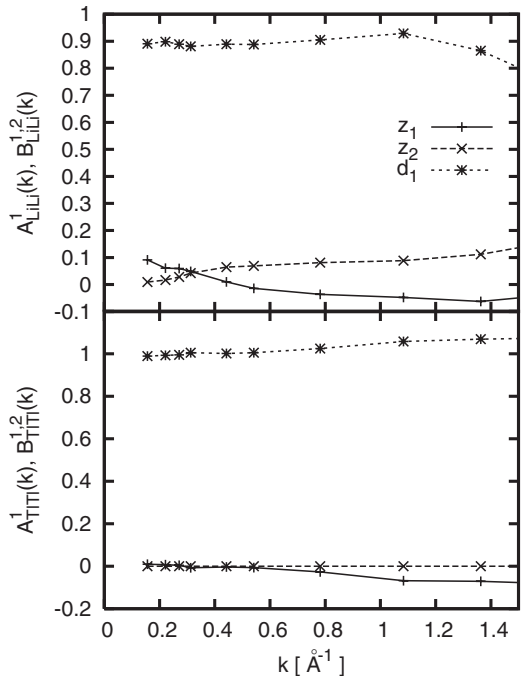

FIG. 13. Wave-number-dependent mode-strengths [Eq. (8)] of the low- and high-frequency collective excitations, $z_1(k)$ and $z_2(k)$, and of the slowest relaxation process $d_1(k)$ in the partial dynamic-structure factors $S_{ii}(k,\omega)$, i=Li,Tl.

$k<0.4$ Å^{-1}, we observe a completely different tendency; the low-frequency branch contribution gets stronger with decreasing wave numbers, illustrating the leading contribution from hydrodynamic sound excitations. Hence, we clearly see a transition in mode contributions from the two branches of propagating excitations. Namely, the low-frequency propagating excitations, which are the ordinary acoustic modes define the side peak of total dynamic-structure factor only in the long-wavelength range, in complete agreement with hydrodynamic theory. Hence, our results clearly indicate that fast sound excitations in Li_4Tl do, in fact, not exist. For $k>0.4$ Å^{-1}, the high-frequency branch defines the dispersion of the side peak of the total dynamic-structure factor. But, towards the long-wavelength range, its contribution vanishes and is replaced by the leading contribution of the hydrodynamic acoustic modes. This implies that a hypothetic linear dispersion of a collective excitation of a fast sound kind does not make any sense in Li_4Tl for $k<0.4$ Å^{-1}.

In the bottom frame of Fig. 12, the mode strengths of the hydrodynamic diffusive relaxation processes $d_1(k)$ and $d_2(k)$ are shown. As this is for hydrodynamic processes, the mode strengths of $d_1(k)$ and $d_2(k)$ must tend to nonzero values in the long-wavelength limit. One can check the long-wavelength asymptotes of calculated mode strengths by using the generalized thermodynamic quantities reported in Fig. 5. From these asymptotes, we obtain the following estimations: $\delta\approx-0.35$, $Z/k_BT\approx17.5$, $C_P\approx3.8k_B$, $C_V\approx3.4k_B$, $\gamma=C_P/C_V\approx1.12$, and $\alpha_T T\approx0.1$. Inserting these values into Eq. (9), one obtains a Landau-Placzek ratio of 0.44. On the other hand, we can evaluate the ratio of mode strengths [Eq. (9)], having estimated $B_{tt}\approx0.7$ and $A^1_{tt}+A^2_{tt}\approx0.3$ from Fig. 12. This leads to a value of ≈0.43, that is in very good agreement with the one estimated via the thermodynamic quantities.

Since fast sound excitations were originally suggested from a study of partial dynamic-structure factors $S_{ii}(k,\omega)$ for the molten alloy Li_4Pb, we now report an analysis of the leading mode contributions to the partial dynamic-structure factors $S_{\mathrm{LiLi}}(k,\omega)$ and $S_{\mathrm{TlTl}}(k,\omega)$. In Fig. 13, we show the mode strengths of both propagating modes and of the slowest relaxation process, $d_1(k)$. The main contribution to the central peak of the partial dynamic-structure factors for $k<1$ Å^{-1} comes from the slowest relaxation process connected with the mutual diffusivity, in complete agreement with Fig. 3 showing partial density-density time-correlation functions. The contributions from propagating modes to $S_{\mathrm{TlTl}}(k,\omega)$ (partial dynamic-structure factor of the heavy particles) are negligible in the long-wavelength range. However, in the case of the partial dynamic-structure factor of the light component, $S_{\mathrm{LiLi}}(k,\omega)$, we obtain a transition in leading mode contribution to the Brillouin peak from the high-(cross symbols) and low-frequency (plus symbols) collective excitations similar as observed for the total dynamic-structure factor $S_{tt}(k,\omega)$. The contribution from the high-frequency branch decays to zero towards small wave numbers, where the low-frequency branch becomes responsible for the side peak of $S_{\mathrm{LiLi}}(k,\omega)$, as it should be in the hydrodynamic limit. These wave-number dependences of mode contributions to the partial dynamic-structure factor of the light component explain why numerical analysis of peak positions of partial current spectral functions $C^L(k,\omega)$ resulted in a merger of the two high- and low-frequency dispersion curves in long-wavelength region.[7,8] Without the analysis of mode contributions, one could not estimate whether such a merger of the two dispersion curves really exists in the binary liquids with disparate masses or not.

IV. CONCLUSION

Our study, combining MD simulations and theoretical GCM approach, has enabled us to extract information relevant for our understanding of collective dynamics of molten Li_4Tl. From analysis of MD-derived time-correlation functions, we have obtained the spectrum of collective excitations, the wave-number dependence of nonpropagating relaxation processes, and their contributions to the shape of the time-correlation functions under study. We have shown that the only wave-number range where the high-frequency branch can be imputed exclusively to the light component corresponds to $k>0.4$ Å^{-1}. For smaller wave numbers, the high-frequency branch corresponds to opticlike excitations: it tends to a nonzero frequency and has much stronger damping than the low-frequency branch, what is a specific feature of kinetic (nonhydrodynamic) collective processes.

The important issue of the long-wavelength dispersion of the fast sound has been explained on the basis of the contributions from the low- and high-frequency branches of collective excitations. Indeed, there exists a transition around $k=0.4$ Å^{-1} in the contributions to the total dynamic-structure factor. As a consequence, its side peak stems from different collective excitations depending on the considered wave-

number range. In the long-wavelength domain ($k < 0.4$ Å^{-1}), the leading contribution comes from the hydrodynamic sound excitations, while for larger k values the side peak of $S_{tt}(k,\omega)$ is solely due to the high-frequency branch of kinetic propagating modes. A similar transition has been found for the partial dynamic-structure factors. Consequently, the dispersion formally derived from the side peak positions of $S_{\mathrm{LiLi}}(k,\omega)$ versus wave number and which looks like the dispersion of a fast sound is not a real one, because it corresponds to different collective excitations: hydrodynamic sound at very small wave numbers and kinetic high-frequency propagating modes for $k > 0.4$ Å^{-1}.

ACKNOWLEDGMENTS

T.B. was supported by the Joint SFBRU-RFBR Program under Project No. Φ28.2/037. Allocation time at the Supercomputer Center of National Technical University of Kiev is acknowledged.

[1] J. Bosse, G. Jacucci, M. Ronchetti, and W. Schirmacher, Phys. Rev. Lett. **57**, 3277 (1986).
[2] A. Campa and E. G. D. Cohen, Phys. Rev. Lett. **61**, 853 (1988).
[3] W. Montfrooij, P. Westerhuijs, V. O. de Haan, and I. M. de Schepper, Phys. Rev. Lett. **63**, 544 (1989).
[4] H. E. Smorenburg, R. M. Crevecoeur, and I. M. de Schepper, Phys. Lett. A **211**, 118 (1996).
[5] P. H. K. de Jong, P. Verkerk, C. F. de Vroege, L. A. de Graaf, W. S. Howells, and S. M. Bennington, J. Phys.: Condens. Matter **6**, L681 (1994).
[6] M. Alvarez, F. J. Bermejo, P. Verkerk, and B. Roessli, Phys. Rev. Lett. **80**, 2141 (1998).
[7] R. Fernandez-Perea, M. Alvarez, F. J. Bermejo, P. Verkerk, B. Roessli, and E. Enciso, Phys. Rev. E **58**, 4568 (1998).
[8] E. Enciso, N. G. Almarza, P. Dominguez, M. A. Gonzalez, and F. J. Bermejo, Phys. Rev. Lett. **74**, 4233 (1995).
[9] T. Bryk and I. Mryglod, J. Phys.: Condens. Matter **12**, 6063 (2000).
[10] T. Bryk and I. Mryglod, J. Phys. Condens. Matter **14**, L445 (2002).
[11] T. Bryk and I. Mryglod, Condens. Matter Phys. **7**, 285 (2004).
[12] T. Bryk and I. Mryglod, J. Phys.: Condens. Matter **17**, 413 (2005).
[13] P. Westerhuijs, W. Montfrooij, L. A. de Graaf, and I. M. de Schepper, Phys. Rev. A **45**, 3749 (1992).
[14] Y. Chushak, T. Bryk, A. Baumketner, G. Kahl, and J. Hafner, Phys. Chem. Liq. **32**, 87 (1996).
[15] N. Anento, L. E. Gonzalez, D. J. Gonzalez, Y. Chushak, and A. Baumketner, Phys. Rev. E **70**, 041201 (2004).
[16] E. Enciso, N. G. Almarza, M. A. Gonzalez, F. J. Bermejo, R. Fernandez-Perea, and F. Bresme, Phys. Rev. Lett. **81**, 4432 (1998).
[17] R. Fernandez-Perea, F. J. Bermejo, J. L. Martinez, E. Enciso, and P. Verkerk, Phys. Rev. E **59**, 3212 (1999).
[18] C. Fiolhais, J. P. Perdew, S. Q. Armster, J. M. MacLaren, and M. Brajczewska, Phys. Rev. B **51**, 14001 (1995); **53**, 13193(E) (1996).
[19] J.-F. Wax, R. Albaki, and J.-L. Bretonnet, Phys. Rev. B **65**, 014301 (2001).
[20] E. B. El Mendoub, R. Albaki, I. Charpentier, J.-L. Bretonnet, J.-F. Wax, and N. Jakse, J. Non-Cryst. Solids **353**, 3475 (2007).
[21] J.-F. Wax and N. Jakse, Phys. Rev. B **75**, 024204 (2007).
[22] S. Ichimaru and K. Utsumi, Phys. Rev. B **24**, 7385 (1981).
[23] T. Bryk, I. Mryglod, and G. Kahl, Phys. Rev. E **56**, 2903 (1997).
[24] I. M. Mryglod, I. P. Omelyan, and M. V. Tokarchuk, Mol. Phys. **84**, 235 (1995).
[25] N. H. March and M. P. Tosi, *Atomic Dynamics in Liquids* (Macmillan, London, 1976).
[26] T. Bryk and I. Mryglod, Condens. Matter Phys. **7**, 15 (2004).
[27] A. B. Bhatia, D. E. Thornton, and N. H. March, Phys. Chem. Liq. **4**, 97 (1974).
[28] T. Scopigno, G. Ruocco, and F. Sette, Rev. Mod. Phys. **77**, 881 (2005).
[29] G. Ruocco and F. Sette, Condens. Matter Phys. **11**, 29 (2008).
[30] C. Cohen, J. W. H. Sutherland, and J. M. Deutch, Phys. Chem. Liq. **2**, 213 (1971).
[31] T. Bryk and I. Mryglod, Condens. Matter Phys. **11**, 139 (2008).
[32] T. Bryk and I. Mryglod, Phys. Rev. E **64**, 032202 (2001).
[33] I. M. Mryglod, Condens. Matter Phys. **1**, 753 (1998).
[34] T. Bryk and I. Mryglod, J. Phys.: Condens. Matter **13**, 1343 (2001).